Multiaxial ratcheting-fatigue behaviors of Sn-3Ag-0.5Cu solder

Ting LIANG, Yongfeng LIANG, Gang CHEN, Xu CHEN

School of Chemical Engineering and Technology, Tianjin University, 300072, China.
Fax: +86-22-27408399, E-mail: xchen@tju.edu.cn

ABSTRACT. *A series of multiaxial ratcheting-fatigue interaction tests have been carried out on Sn-3Ag-0.5Cu lead-free solder specimens. All tests were conducted under cyclic shear strain with the constant axial stress at the room temperature with the shear strain rate of* 5×10^{-3}*/s. It was found that the ratcheting strain increased with increasing axial stress and shear strain amplitude while the fatigue life decreased at the same time. The ratcheting strain rate was linear with axial stress in double logarithmic coordinate. The Gao-Chen model which adopted the maximum shear strain and the ratcheting strain rate as the damage parameter predicted the multiaxial ratcheting fatigue life well.*

INTRODUCTION

The lead-free solder is widely used in the electronic packaging industry instead of the lead solder because the lead solder will affect the environment and human health seriously [1]. Ratcheting effect has drawn more and more attention from researchers recently. The effect factors of ratcheting deformation have been studied [2-7], such as loading rate, mean stress, stress amplitude, loading path, loading history, temperature and material properties. As for ratcheting behavior in lead-containing and lead-free solders, Chen et al. [8, 9], Kobayashi and Sasaki [10] have studied uniaxial ratcheting behaviors on solder alloys. Date et al. [11], Liu et al. [12], Lim et al. [13], Gao and Chen [14] have studied how the ratcheting effect influence the fatigue life for lead-free solder Sn-3.5Ag .

In this study, a series of multiaxial ratcheting-fatigue tests were conducted on Sn-3Ag-0.5Cu lead-free solder. The Gao-Chen model for life prediction in multiaxial low cycle fatigue was applied and the prediction of fatigue life with ratcheting will be discussed.

MATERIALS AND EXPERIMENT PROCEDURE

The material used in this study was lead-free solder Sn-3Ag-0.5Cu. Its chemical composition is shown in Table 1. The dimensions of the specimen are shown in Fig. 1. The specimens were cooled to room temperature in furnace after heated at 146°C (0.85 times the melting point) for three hours and then placed at room temperature for a month to release residual stress. Due to the low hardness of the solder and small dimension of the specimen, two stainless steel tube protectors were glued to both ends of the specimen to avoid damage from the collet of the test machine. All the tests were carried out with a micro type tension-torsion fatigue testing machine, and the data collection was made using an automatic data acquisition system. Both the test machine and the data acquisition system were developed by CARE Lab, Tianjin University. All the multiaxial tests were conducted under axial stress control and torsion angle control at room temperature.

Table 1. Chemical compositions of Sn-3Ag-0.5Cu (wt.%)

Solder type	Ag	Cu	Sb	Fe	As	Ni	Cd	Al	Zn	Pb	Sn
Sn-3Ag-0.5Cu	3.0	0.5	<0.05	<0.02	<0.03	0.01	<0.002	<0.002	<0.002	<0.08	Bal.

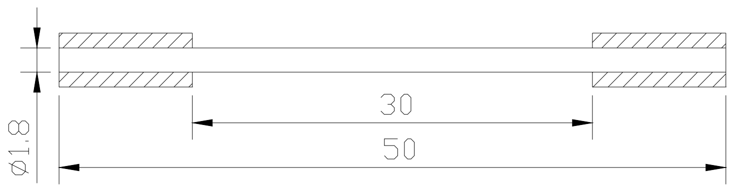

Figure 1. Specimen geometry (unit: mm).

In this study, the shear stress is defined as the method of Miller and Chandler[15]:

$$\tau = \frac{1}{2\pi R^3}\left[3T + \gamma \frac{dT}{d\gamma}\right] \tag{1}$$

where τ is the shear stress, R is the radius of specimen, T is the torque, γ is the shear strain. Applying the perfect elastic-plastic model and assuming the cross section of specimen keeping planar during torsion, the shear stress is obtained:

$$\tau = \frac{3T}{2\pi R^3} \tag{2}$$

The shear strain is defined as:

$$\gamma = \frac{\pi \alpha R}{180L} \tag{3}$$

where L is the specimen length, α is the torsional angle.

The ratcheting strain is defined as:

$$\varepsilon_r = \frac{\varepsilon_{\max} + \varepsilon_{\min}}{2} \tag{4}$$

where $\varepsilon_{\max}$ and ε_{min} are the maximum axial strain and minimum axial strain respectively in a cycle.

The ratcheting strain rate is defined as:

$$\dot{\varepsilon}_r = d\varepsilon_r / dN \tag{5}$$

where N is the number of cycle.

EXPERIMENT RESULTS AND DISCUSSIONS

Before analysis of multiaxial ratcheting-fatigue interaction, uniaxial tensile tests and pure torsional tests under different strain rates were performed to obtain the mechanical properties of Sn-3Ag-0.5Cu, respectively. The yield stress, tensile strength, yield shear stress, shear strength are rate dependent. The specimens were tested under constant axial tensile load and triangular cyclic torsional load in multiaxial ratcheting-fatigue procedure. The loading path is shown in Fig. 2. The effects of axial stress and shear strain amplitude on the ratcheting strain and fatigue life were investigated in this study.

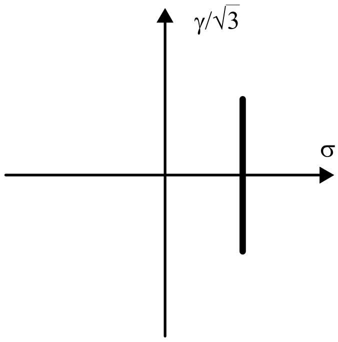

Fig. 2. Loading path in multiaxial fatigue test.

Analysis of Multiaxial Ratcheting Strain

Figure 3 indicates that the constant axial load little affect the shear stress-strain hysteresis loop. The maximum shear stress under different axial load is similar to be constant.

The relation between ratcheting strain and number of cycles was shown in Fig. 4 where the effect of axial stress and shear strain amplitude on the ratcheting strain can be observed respectively. The ratcheting strain increased with increasing axial stress and shear strain amplitude respectively. The failure ratcheting strain is about in the range of

20%~30%. Figure 4 shows that the ratcheting strain occurred in axial direction significantly. Under the same shear strain amplitude, the higher axial stress caused the larger ratcheting strain and lower cycles to failure. The relation between ratcheting strain and number of cycles to failure was divided into two ranges: the range with constant ratcheting strain rate which almost covered the entire fatigue life and the range with accelerative ratcheting strain rate followed by fatigue fracture which occurred in a short time in most tests. There was no trend of ratcheting shakedown in all tests.

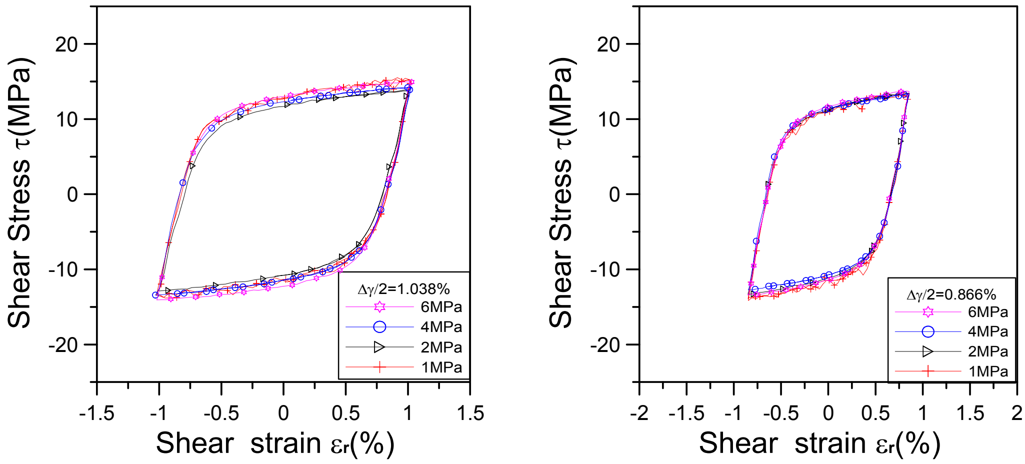

(a) (b)

Fig. 3. Cyclic stress-strain hysteresis loops.

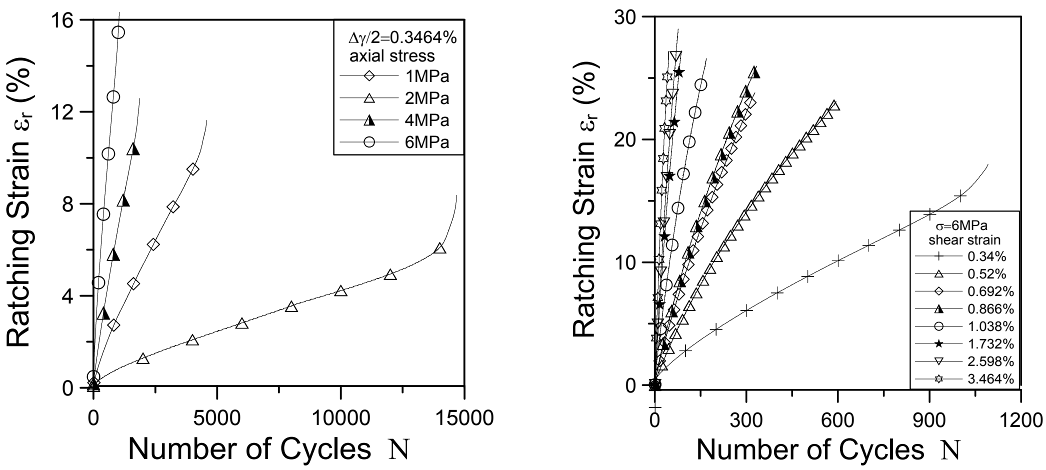

(a) (b)

Fig 4. Ratcheting strain with cycles under different axial stresses and shear strains amplitudes.

The relation between ratcheting strain rate and axial stress was shown in Fig. 5 in the log-log coordinate. It can be seen that the ratcheting strain rate increased with the increasing axial stress. The approximate linear relations in the figure, which indicated the constant axial ratcheting strain rate, supported the model proposed by Gao and Chen [14] which combined the saturation axial ratcheting strain rate as the damage parameter to predict the ratcheting-fatigue life.

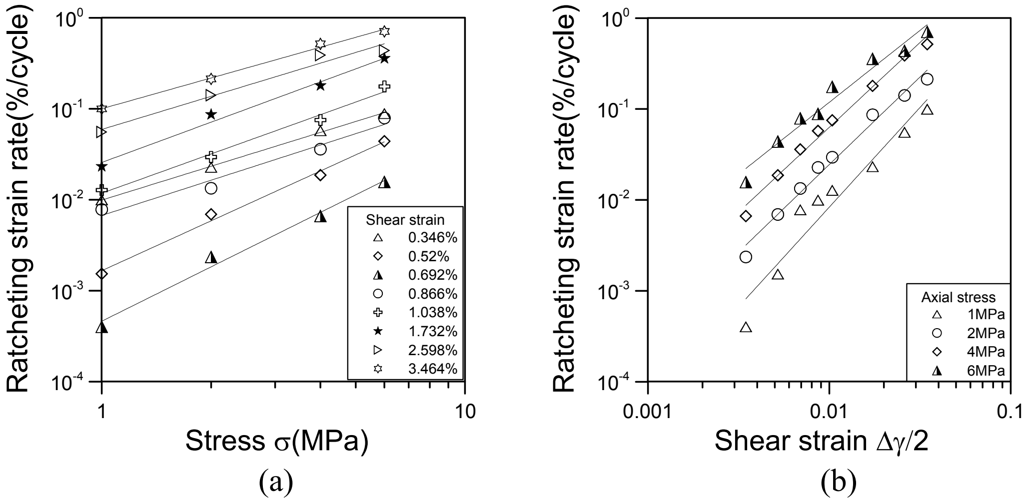

Fig 5. Relation between ratcheting strain rate and (a)axial stress; (b)shear strain amplitude.

Analysis of Multiaxial Ratcheting-Fatigue Life

Figure 6 shows the relation between shear stress amplitude and number of cycles to failure under different axial stresses. The curves were divided into two phases: the shear stress amplitude decreased with constant rate in the first phase which covered the most fatigue life and the shear stress amplitude decreased sharply in the second phase which followed by fatigue fracture.

Figure 7 shows the linear relation between the shear plastic strain amplitude and the fatigue life which could be described by Solomon equation [16]:

$$\frac{\Delta\gamma_p}{2} = \gamma_f'(2N_f)^{c_0} \tag{6}$$

where $\Delta\gamma_p$ is the plastic shear strain range, N_f is the fatigue life, γ_f' is the fatigue ductility coefficient, c_0 is the material parameter. The fit parameters are shown in Table 2 which indicate the similarity of c_0 and the variation of γ_f' for different axial stresses σ.

Table 2. Experimental values for constants c_0 and γ_f'

σ(MPa)	0	1	2	4	6
c_0	-0.6345	-0.6333	-0.6589	-0.6826	-0.7106
γ_f'	2.7836	1.3189	0.9922	0.6813	0.5711

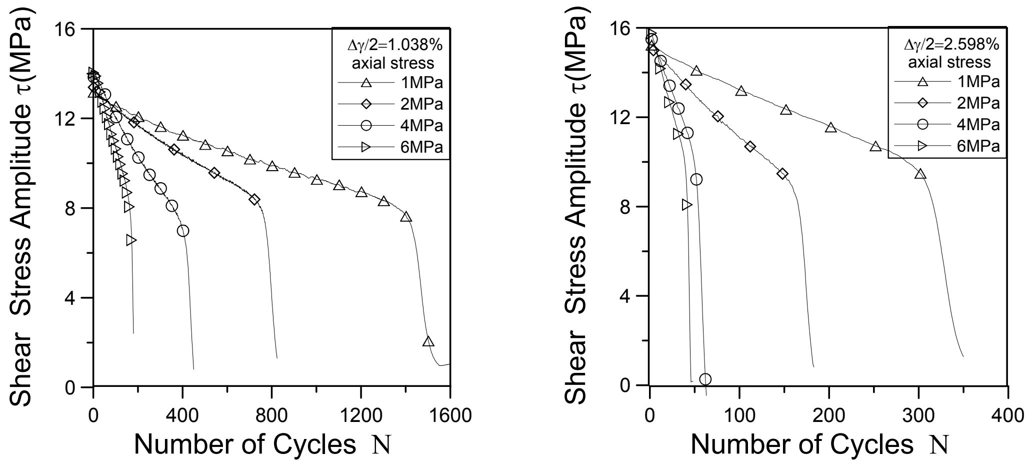

Fig. 6. Shear stress amplitude with cycles.

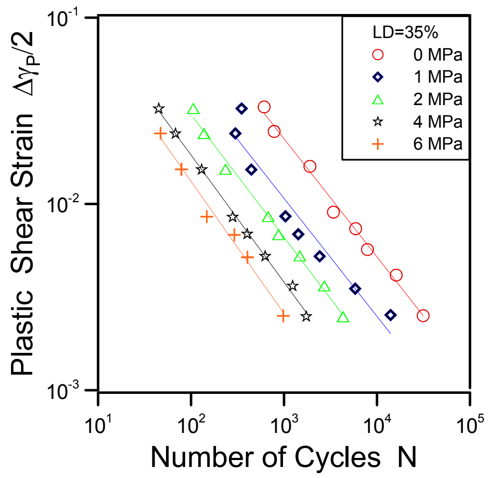

Fig 7. Relation between shear plastic strain amplitude and fatigue life.

LIFE PREDICTION OF MULTIAXIAL RATCHETING FATIGUE

Gao and Chen [14] conducted a series of multiaxial ratcheting fatigue tests on Sn-3.5Ag and proposed a model with the maximum shear strain $\Delta\gamma_{max}$ and axial ratcheting strain rate $\dot{\varepsilon}_r$ as the damage parameters:

$$\frac{\Delta\gamma_{max}}{2} + S\dot{\varepsilon}_r^{-c_0} = \frac{\tau_f'}{G}(2N_f)^{b_0} + \gamma_f'(2N_f)^{c_0} \quad (7)$$

where b_0 is the torsional fatigue intensity exponent, c_0 is the torsional fatigue ductility exponent, S is the constant obtained from the uniaxial tests. This model was used to predict the fatigue life of Sn-3Ag-0.5Cu in this work where b_0=-0.103, c_0=-0.6345, τ_f'=24.1098 MPa, γ_f'=2.7836, S=0.2. The prediction results are shown in Fig. 8.

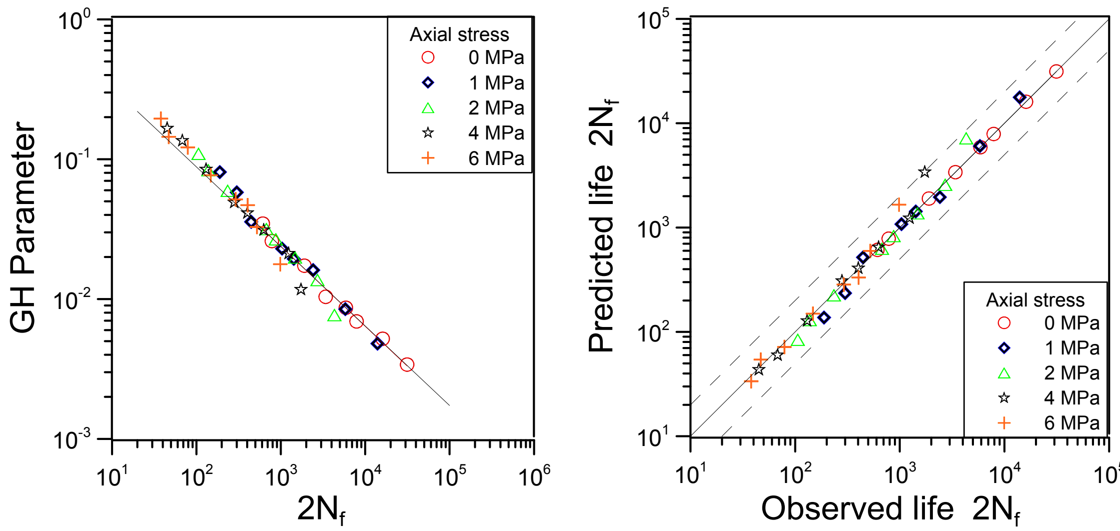

Fig. 8. Fatigue life prediction based on Gao-Chen model.

The first term in left equation reflected the influence on fatigue life of shear strain amplitude and the second term reflected the influence of axial stress. The Gao-Chen model predicted the multiaxial ratcheting fatigue life within the bound of factor of two. The satisfactory result is due to the combination of the axial ratcheting effect and the fatigue life while the ratcheting strain rate shows power relationship with the fatigue life.

CONCLUSIONS

A series of multiaxial ratcheting fatigue test were carried on Sn-3Ag-0.5Cu solder in this work and the fatigue life was predicted with the method considered ratcheting effect. The conclusions are obtained as follows:

1. Axial stress influences little peak shear stress response. The axial ratcheting strain increases with increasing axial stress and shear strain amplitude. The ratcheting strain rate is linear with axial stress in double logarithmic coordinate. The fatigue life decreases rapidly with the increasing axial stress and shear strain amplitude.

2. The Gao-Chen model with the maximum shear strain $\Delta\gamma_{max}$ and axial ratcheting strain rate $\dot{\varepsilon}_r$ as the damage parameter predicts the multiaxial ratcheting fatigue life of Sn-3Ag-0.5Cu solder well.

Acknowledgments: The authors are grateful for the financial support from the National Natural Science Foundation of China (No.11072171).

Reference

1. Zeng, K., Tu, K.N., (2002) *Materials Science and Engineering* **R38**, 55-105.
2. Jiang, Y.Y., Sehitoglu, H., (1994) *Int. J. Plast.* **10(5)**, 579-608.
3. Sakane, M., Inoue, A., Chen, X., Kim, K.S., (2007) *ASME PVP* **1**, 385-391.
4. N. Ohno, J.D. Wang, (1993) *Int. J. Plast*. **9**, 375-390.
5. Kan, Q.H., Kang, G.Z., Zhang, J., Sun, Y.F, (2006) *Nuclear Power Engineering* **27(2)**, 59-63.
6. Zhang, Z.,Chen X., (2009) *Polym. Test.* **28(3)**, 288-295.
7. Hassan, T., Kyriakides, S., (1994) *Int. J. Plast*. **10,** 149-184.
8. Chen, X., Yu, D.H., Kim, K.S., (2005) *Mater. Sci. Eng., A* **406(1-2)**, 86-94.
9. Chen, G., Chen, X., Niu, C.D., (2006) *Mater. Sci. Eng., A* **421(1-2**), 238-244.
10. Kobayashi, T., Sasaki, K., (2009) *J. Mater. Sci. - Mater. Electron*. **20(4)**, 343-353.
11. Date, S, Ishikawa, H, Otani, T, Takahashi, Y. (2008) *Nucl. Eng. Des.* **238**, 336-346.
12. Liu, Y.J., Kang, G.Z., Gao, Q., Li, Z., (2008), *Engineering Mechanics* **25(11)**, 186-191.
13. Lim, C.B., Kim, K.S., Seong, J.B., (2009) *Int. J. Fatigue* **31(3)**, 501-507.
14. Gao, H., Chen, X**.**, (2009) *Int. J. Fatigue* **31(2)**, 276-283.
15. Miller, K.J., Chandler, D.C., (1970) *Proc Inst Mech Eng* **2(4)**:262–70.
16. Solomon, H.D., (1991) *J. Electron Packaging* **113**, 102-108.